AGU PUBLICATIONS

Geophysical Research Letters

RESEARCH LETTER
10.1002/2013GL058928

**Key Points:**
- Performance of CMIP5 in describing global statistics of the atmosphere
- Biases larger than 20
- No change in the statistics of the baroclinic and planetary-scale motions

**Supporting Information:**
- Readme
- fs02.eps
- fs01.eps

**Correspondence to:**
S. Calmanti,
sandro.calmanti@enea.it

**Citation:**
Di Biagio, V., S. Calmanti, A. Dell'Aquila, and P. M. Ruti (2014), Northern Hemisphere winter midlatitude atmospheric variability in CMIP5 models, *Geophys. Res. Lett.*, *41*, 1277–1282, doi:10.1002/2013GL058928.

Received 2 DEC 2013
Accepted 2 FEB 2014
Accepted article online 7 FEB 2014
Published online 20 FEB 2014

# Northern Hemisphere winter midlatitude atmospheric variability in CMIP5 models

**Valeria Di Biagio[1], Sandro Calmanti[2], Alessandro Dell'Aquila[2], and Paolo M. Ruti[2]**

[1]Sapienza University of Rome, Rome, Italy, [2]ENEA-UTMEA, Agenzia nazionale per le nuove tecnologie, l'energia e lo sviluppo economico sostenibile, Rome, Italy

**Abstract** The Northern Hemisphere midlatitude winter atmospheric variability simulated by Coupled Model Intercomparison Project phase 5 (CMIP5) models is analyzed at spatial and temporal scales corresponding to the growth of baroclinic eddies and planetary waves. We use a global scalar metric of the wave energy frequency-wave number spectrum to identify potential improvements of the CMIP5 ensemble compared to previous coordinated model simulations (CMIP3). We also evaluate whether CMIP5 models predict future shifts in the global baroclinic eddies and planetary-scale wave activities. With respect to CMIP3, no significant improvements are found, thereby suggesting that no significant breakthrough in the modeling of the climate system has been hit over the last few years. No significant changes are found in RCP4.5 scenarios for the selected metric of the baroclinic and planetary-scale atmospheric flows, thus indicating that localized changes with potential societal impact might not be related to changes in key fundamental properties of the atmospheric circulation.

## 1. Introduction

Baroclinic instability and planetary standing waves in the midlatitudes are a key component of the climate system since they move the largest component of the poleward heat and momentum transport [*Czaja and Marshall*, 2006]. Therefore, the ability to correctly simulate the statistical properties of midlatitude atmospheric circulation is a critical requirement for climate models. Early studies conducted on numerical weather prediction models [*Tibaldi*, 1986] and, later, works on Coupled Model Intercomparison Project phase 3 (CMIP3) models [*Lucarini et al.*, 2007] showed a tendency to overestimate baroclinic short wave energy and to underestimate the amplitude of planetary waves.

The recent development of a new set of climate simulations under the CMIP5 framework [*Taylor et al.*, 2012], which contributed to the science basis for the Fifth Assessment Report of the Intergovernmental Panel on Climate Change, allows for a comparative analyses of the overall improvements in our ability to simulate different aspects of the climate system [*Knutti et al.*, 2013]. For example, *Zappa et al.* [2013] found a general improvement in the simulation of the North Atlantic extratropical storm tracks and *Colle et al.* [2013] has suggested that this improvement might be related to the adoption of a higher horizontal resolution in some of the CMIP5 models. According to *Chang* [2013], CMIP5 models mostly simulate too weak and too equatorward storm tracks. They also found an upper troposphere signal of a poleward shift and increasing strength of the storm tracks toward the end of the 21st century in the Northern Hemisphere. Moreover, according to *Mizuta* [2012], the frequency of intense cyclones will increase on the polar side of the storm tracks, especially in the North Pacific, a result which seems to depend on the definition of extratropical cyclone dynamical intensity [*Chang*, 2012].

Building on the analysis done by *Lucarini et al.* [2007] on the CMIP3 simulations, we consider here the new CMIP5 ensemble and we analyze the winter (December-January-February (DJF)) baroclinic and standing waves in the midlatitudes by focusing on suitably defined model metrics. The main objective is to identify possible improvements in the ability to simulate atmospheric circulation variability at spatial and temporal scales which can be linked to well-defined physical drivers, namely, the growth and equilibration of baroclinic instabilities and the interaction of large-scale atmospheric flows with orography and with zonal asymmetries in atmospheric convection. The new CMIP5 ensembles has been depicted as a "better CMIP3," rather than a radically new ensemble [*Knutti and Sedláček*, 2012], thereby highlighting that in spite of the consistency and robustness of result compared to previous modeling efforts, major milestones in the development of climate models have not been hit.

  

**Table 1.** Overview of the CMIP5 Models Atmosphere and Ocean Resolutions[a]

| ID | Model | Atmosphere Resolutions | Ocean Resolutions |
|---|---|---|---|
| 1 | CanESM2 | T63, L35 | ∼0.94° latitude × 1.4° longitude, L40 |
| 2 | CMCC-CM | T159, L31 | 0.5°-2° latitude × 2° longitude, L31 |
| 3 | CNRM-CM5 | T127, L31 | 1/3°-1° latitude × 1° longitude, L42 |
| 4 | CSIRO-Mk 3.6.0 | T63, L18 | ∼0.94° latitude × 1.875° longitude, L31 |
| 5 | FGOALS-g2 | 3° latitude × 2.8° longitude, L26 | ∼1° latitude × 1° longitude, L30 |
| 6 | GFDL-CM3 | ∼200km, L48 | Tripolar ∼1/3° -1 latitude × 1° longitude, L50 |
| 7 | GFDL-ESM2G | 2° latitude × 2.5° longitude, L24 | Tripolar ∼1/3° -1 latitude × 1° longitude, L63 |
| 8 | GFDL-ESM2M | 2° latitude × 2.5° longitude, L24 | Tripolar ∼1/3° -1 latitude × 1° longitude, L50 |
| 9 | HadGEM2-ES | 1.25° latitude × 1.875° longitude, L38 | 1/3°-1° latitude × 1° longitude, L40 |
| 10 | INM-CM4 | 1.5° latitude × 2° longitude, L21 | 0.5° latitude × 1° longitude, L40 |
| 11 | IPSL-CM5A-LR | 1.875° latitude × 3.75° longitude, L39 | ∼0.5°-2° latitude × 2° longitude, L31 |
| 12 | MIROC5 | T85, L40 | ∼0.5°-1.4° latitude × 0.8° longitude, L50 |
| 13 | MIROC-ESM | T42, L80 | ∼0.5°-1.7° latitude × 1.4° longitude, L44 |
| 14 | MIROC-ESM-CHEM | T42, L80 | ∼0.5°-1.7° latitude × 1.4° longitude, L44 |
| 15 | MPI-ESM-LR | T63, L47 | Bipolar ∼1.5° latitude × 1.5° longitude, L40 |
| 16 | MPI-ESM-MR | T63, L95 | Tripolar ∼0.4° latitude × 0.4° longitude, L40 |
| 17 | MRI-CGCM3 | TL159, L48 | 0.5° latitude × 1° longitude, L51 |
| 18 | NorESM1-M | 1.9° latitude × 2.5° longitude, L26 | Bipolar ∼ 1° latitude × 1° longitude, L53 |

[a]The NCEP reanalysis has resolution: 2.5° latitude × 2.5° longitude, L28.

Instead of focusing on the improvements in the description of local features of the atmospheric circulation, such as the location and extension of the North Atlantic storm track, we present a complementary analysis of the performance of CMIP5 in describing global statistical properties of the atmospheric circulation which are essentially connected to the meridional heat transport [*Lucarini and Ragone*, 2011].

In particular, as the climate system should obey general energy balance constraints, climate models are also to provide an accurate description of the processes that maintain the equator-to-pole energy transport, thereby balancing the latitudinal differences between incoming and outgoing radiation.

We also analyze future projected changes of baroclinic and standing waves. In particular, we conduct this analysis in the framework of the European Union project IMPACT2C. The aim of the project is to quantify the impact of an increase of global surface temperature of 2°C above the preindustrial level. We, therefore, consider future projections over the period 2058–2080 when most of the RCP4.5 scenarios reach the +2°C threshold. The objective of the analysis is to establish if the projected changes in regional climate, such as those discussed by *Zappa et al.* [2013] and *Mizuta* [2012] are also reflected into the fundamental statistical properties of the atmospheric circulation.

## 2. Data and Methods

We use the CMIP5 distributed archive of global climate model simulations, and we consider the model listed in Table 1 for the period 1979–2001 for historical runs and the period 2058–2080 for RCP4.5 simulations (broadly corresponding to an increase of 2°C in the global surface temperature above the preindustrial level). As in *Lucarini et al.* [2007], we use the December-January-February (DJF) daily meridional wind data at 500 hPa to derive an integral metric of the corresponding geopotential height, averaged over the latitudinal belt 30°N–75°N, where the bulk of the baroclinic and of the low-frequency waves activity is observed, as discussed in *Dell'Aquila et al.* [2005].

We adopt the spatiotemporal spectral decomposition introduced originally by *Hayashi* [1979] and then modified by *Pratt* [1976] and *Fraedrich and Bottger* [1978] to address the issue of low coherence in the region of the spectrum with low frequency and low wave number, in which standing waves are expected. This method was already adopted in previous analyses of midlatitude circulation [*Lucarini et al.*, 2007; *Dell'Aquila et al.*, 2005]. We consider the quantities $H^n_{\mathrm{TOT}}(k_j,\omega_m)$, $H^n_{E/W}(k_j,\omega_m)$, $H^n_{\mathrm{ST}}(k_j,\omega_m)$ which represent, for each $n$th year and for each wavelength-frequency pair $(k_j,\omega_m)$, the total atmospheric variance, the propagating eastward/westward components, and the standing component, respectively. We use these quantities to define an integral metric of the energy of baroclinic and standing waves. In particular, the energy $E_{\mathrm{Baroc}}$ of the baroclinic waves, i.e., the synoptic traveling waves associated with the release of available energy driven by conventional baroclinic conversion [*Blackmon*, 1976; *Speranza*, 1983; *Wallace et al.*, 1983], is computed by integrating the eastward propagating component over the high frequency high wave number,

  

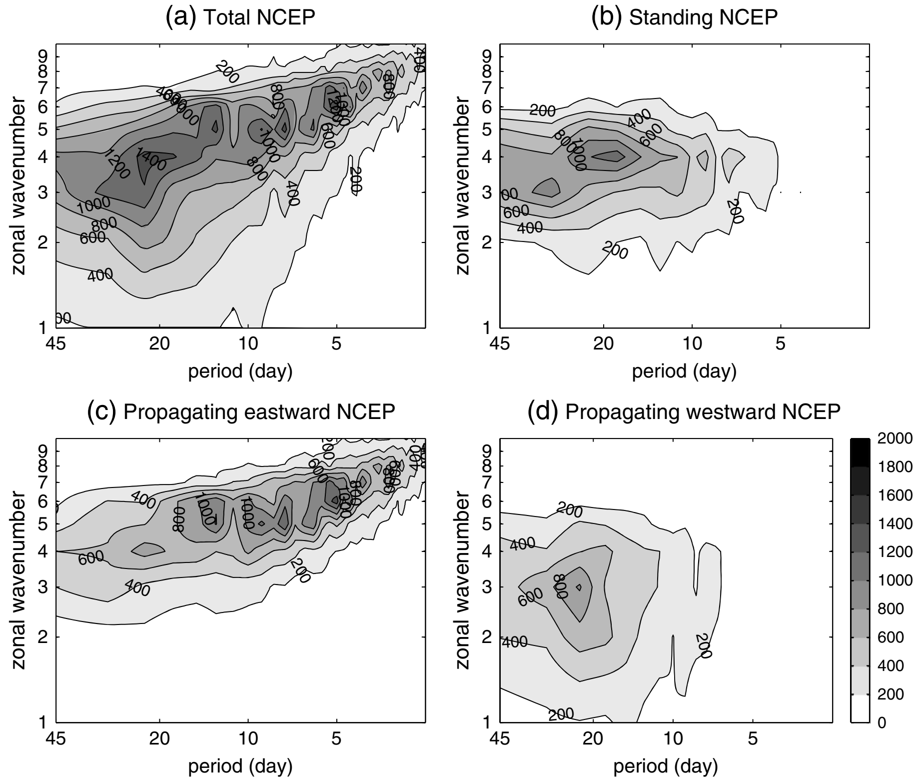


**Figure 1.** (a–d) Climatological average over 22 winters of Hayashi spectra for DJF geostrophically reconstructed geopotential height at 500 hPa, in the latitudinal belt 30°N–75°N, from NCEP meridional wind. The Hayashi spectra have been obtained by multiplying the spectra by $k_j\omega_m\tau/(2\pi)$, $\tau = 90$ days so that equal geometrical areas represent equal variance in log-log plots, and their units are square meter. The LFLW standing and the HFHW eastward propagating areas are indicative of the planetary and the baroclinic waves activities, respectively.

corresponding to 2–7 days and to zonal wave numbers greater than 6. The energy $E_{\mathrm{Plan}}$ of the planetary waves that interact with orography [*Charney and De Vore*, 1979; *Charney and Straus*, 1980; *Benzi et al.*, 1986] and that are catalyzed by the subtropical jet [*Benzi and Speranza*, 1989; *Ruti et al.*, 2006] is instead computed by integrating the standing component over the low frequency low wave number, corresponding to 10–45 days and to zonal wave numbers between 2 and 4.

The indices $< E_{\mathrm{Baroc}} >$ and $< E_{\mathrm{Plan}} >$ are computed both for historical and for RCP4.5 simulations by averaging the indices over the corresponding time intervals. The historical simulations are compared to the corresponding quantities obtained by the National Centers for Environmental Prediction (NCEP) [*Kistler et al.*, 2001] and the ERA-Interim [*Dee et al.*, 2011] reanalyses. Then RCP4.5 simulations are compared with the historical ones to discuss the projected changes in baroclinic and in the planetary standing waves.

An additional indicator of the midlatitude variability is computed by following the same spectral decomposition procedure used so far, but without the meridional averaging over the considered latitudinal belt. The aim of this analysis is to assess whether CMIP5 models predict any meridional future shift in the bulk of the baroclinic and planetary-scale waves.

## 3. Results

The reference spatiotemporal spectra averaged over the 22 winters included in the NCEP data set spanning the time period 1979–2001 are represented in Figures 1a–1d. This spectral decomposition of atmospheric circulation pattern is similar to the previous analysis on CMIP3 models already cited [*Lucarini et al.*, 2007]. A large portion of the total variance is concentrated in the low frequency low wave number (LFLW) domain, and it can be related mostly to standing waves and to westward propagating waves. The high frequency high wave number (HFHW) domain, corresponding mainly to synoptic disturbances, contains a smaller portion of the total variance, and it is almost exclusively related to eastward propagating waves. In contrast, the average spectrum of westward propagating variance, mainly due to long and low-frequency waves, does

  

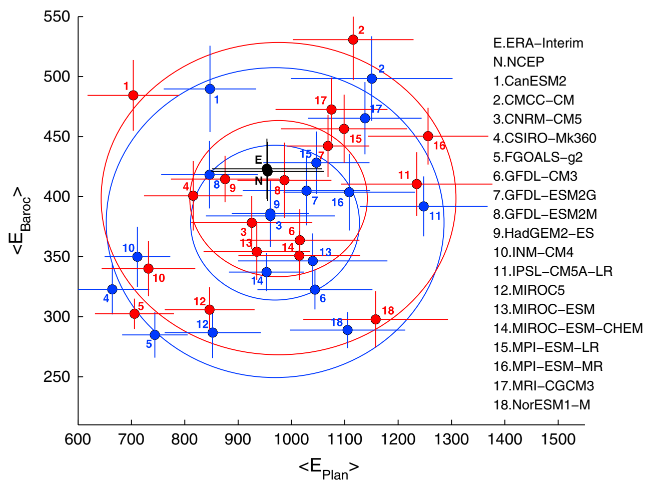


**Figure 2.** Scatterplot of $<E_{\mathrm{Baroc}}>$, for the baroclinic waves versus $<E_{\mathrm{Plan}}>$, for the planetary waves, computed for the $Z$ 500 hPa DJF data averaged in the latitudinal belt 30°N–75°N, by the CMIP5 historical runs (blue) and RCP4.5 simulations (red). The letters $N$ and $E$ indicate the NCEP reanalysis and the ERA-Interim one, respectively. For each dot the horizontal (vertical) error bar gives the 95% confidence level of $2\sigma_E/\sqrt{N}$, where $E = E_{\mathrm{Plan}}$ ($E_{\mathrm{Baroc}}$), $N = 22$, and $\sigma_E$ is the standard deviation of the annual values of $E_{\mathrm{Baroc}}$ and $E_{\mathrm{Plan}}$. The inner (outer) ellipse has semiaxes equal to the standard deviation (twice the standard deviation) of the data in the corresponding direction.

not feature a similarly clean and legible structure, suggesting that specific phenomena with well-defined propagation properties may not be distinguished by this method.

The integral quantities $<E_{\mathrm{Baroc}}>$ and $<E_{\mathrm{Plan}}>$ derived from the 18 CMIP5 models for the historical and RCP4.5 simulations are reported in Figure 2. The error bars represent twice the interannual variability (i.e., standard deviation of the mean) computed for the number 22 winters.

Considering the historical simulations (blue dots), planetary and baroclinic wave energy from the CMIP5 models is consistent with the reanalyses (black dots) only for the GFDL-ESM2G and MPI-ESM-LR models; large biases, even larger than 20%, are found in some models. On average, the baroclinic wave energy is typically underestimated and the planetary waves are slightly overestimated by the climate models, in contrast with the already cited study on the CMIP3 models [*Lucarini et al.*, 2007].

The reanalyses are contained in the inner ellipse (within 1 standard deviation from the ensemble mean), with the eight best CMIP5 models. All the other CMIP5 models, except CMCC-CM, CSIRO-Mk360, and FGOALS-g2, are within the outer ellipse (within twice the standard deviation from the ensemble mean). Note that neither a higher vertical nor a higher horizontal resolution necessarily imply a better agreement with observations. In particular, models from the same group (i.e., the GFDL/CM3/ESM2G/ESM2M family and the MPI/ESM-LR/ESM-MR family) show a lower performance in the considered metric in the case of a higher vertical resolution.

In the case of RCP4.5 scenarios (red dots), the dispersion of the model is similar to the historical data, with eight models included in the inner ellipse and all but three models contained in the outer one. The baroclinic activity projected for the scenario is higher than the historical for six models (CSIRO-Mk360, GFDL-CM3, GFDL-ESM2G, HadGEM2-ES, MPI-ESM-LR, and MPI-ESM-MR) and essentially unchanged for the other models. The CMIP5 ensemble mean for the scenario data undergoes a shift of about 4% toward higher baroclinic activity with respect to the historical one. However, the shift is not statistically significant according to a Kolmogorov test at 95% confidence level. In the case of planetary waves, present climate and future projections do not show significant changes for most of the models. In particular, it has been verified (not shown) that this result is not sensitive to the choice of a particular time period, at least for the case of RCP4.5 scenarios.

Overall, considering the small changes and the large spread found between the ensemble members according to the proposed metric, no significant change in the statistical properties of the baroclinic and planetary-scale motions is detected.

The meridional profiles of the baroclinic and planetary wave activity computed from historical and scenario data, averaged over the 18 CMIP5 models for each latitude are shown in Figures 3a and 3b. A slight shift toward higher values is suggested for the baroclinic variability, and a weak decrease of the planetary variability. However, at all latitudes, the baroclinic activity in the historical and in the scenario simulations are compatible with the null hypothesis of having the same distribution of the indices of baroclinic and planetary-scale activity at each latitude, according to a Kolmogorov-Smirnov (K-S) test at a significance level of 5%. Similar results are found for the planetary-scale variability.

  

10.1002/2013GL058928

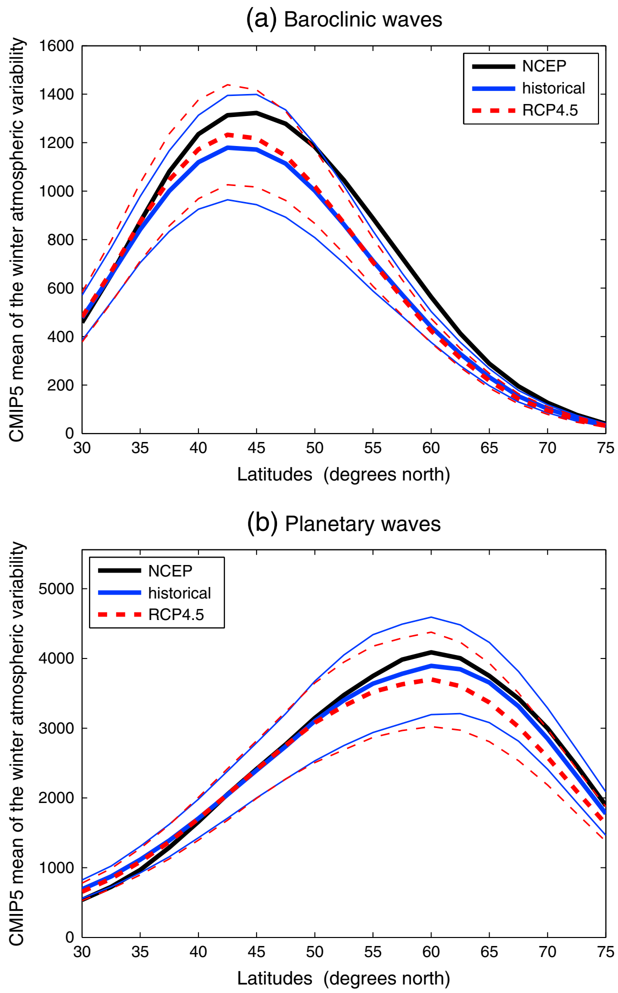


**Figure 3.** Meridional profiles in the belt 30°N–75°N of (a) $< E_{Baroc} >$ of the baroclinic waves and (b) $< E_{Plan} >$ of the planetary waves, averaged on the CMIP5 models for the 1979–2001 historical simulations (blue solid lines), compared with the NCEP reanalysis on the same years (black line), and the 2058–2080 RCP4.5 simulations (red broken lines). In Figures 3a and 3b, for historical and RCP4.5 simulations, the heavy lines represent the mean and the thin lines delimit the variance of the CMIP5 ensemble.

Finally, the distribution of the latitudes at which the maximum baroclinic and planetary wave activity is observed has been considered. Again, a K-S test at 5% confidence level between the historical and the scenario simulation suggests that no significant change occurs in the meridional shift of the maximum wave activity.

## 4. Discussion

We have considered the planetary and baroclinic wave activity simulated by the CMIP5 historical and scenario simulations with the objective of comparing the results with a previous analysis conducted on CMIP3 models and to identify potential changes in future climate projections.

As for the case of CMIP3, the present climate simulations agree with observations (e.g., NCEP reanalysis) only for a few global climate models; large biases, even larger than 20%, are found in several cases.

The historical simulations show that the baroclinic wave energy is slightly underestimated by the climate models, and the planetary waves are slightly overestimated, in contrast with the previous studies on CMIP3 models. However, the multimodel mean is approximately as close to the reanalysis as in the case of CMIP3, thereby suggesting that the systematic component of the misrepresentation of baroclinic and planetary waves is indeed small.

Concerning the RCP4.5 scenarios, a slight shift of the models ensemble can be detected with 4% higher values of the baroclinic waves for the future (2058–2080 years) with respect to the present climate. However, such a shift is not statistically significant as a consequence of the spread in the behavior of the considered models.

Our results are in agreement with the analyses of extratropical circulation conducted with different methodologies. As in *Chang* [2012], we observe weak tendency of CMIP5 models to underestimate high-frequency variability. Concerning the trends, we find a small, although not statistically significant, increase in the baroclinic waves activity for RCP4.5 scenario, in agreement with *Chang* [2013].

With the integral metric of the baroclinic and planetary-scale wave activity adopted in this study, even the models that are in close agreement with observations do not show the same sign of the tendency in the future scenario. Note that the adopted metric does not account for the longitudinal phase of the wave activity, and therefore, our results do not rule out the possibility that the considered models produce localized future changes with even severe societal impacts. However, the small (not statistically significant) changes in future baroclinic and planetary-scale activity are in a qualitative agreement with the findings of *Zappa* *et al.* [2013] and *Mizuta* [2012]) who also report limited future changes at the regional scale and significant disagreements among the models.

This work shows that in spite of significant improvements in the ability to simulate aspects of the climate system that are important for their potential societal impact [*Knutti et al.*, 2013], work is still required to achieve a better simulation of simple yet fundamental properties of the midlatitude atmospheric dynamics that cannot be improved by focusing on specific characteristics of the modeling systems such as the model resolution or on the use of specific parameterization schemes.

**Acknowledgments**
The authors wish to thank Valerio Lucarini for useful discussions and acknowledge the World Climate Research Programme Working Group on Coupled Modelling, which is responsible for CMIP, and the climate modeling groups for producing and making available their model output. For CMIP, the U.S. Department of Energy Program for Climate Model Diagnosis and Intercomparison provides coordinating support and led the development of software infrastructure in partnership with the Global Organization for Earth System Science Portals. This work has been supported by the EU-FP7 projects IMPACT2C, SPECS and by the DTA-MIUR NextData Project. The comments of two anonymous reviewers helped us to improve the clarity of the manuscript.

The Editor thanks two anonymous reviewers for their assistance in evaluating this paper.

## References

Benzi, R., P. Malguzzi, A. Speranza, and A. Sutera (1986), The statistical properties of general atmospheric circulation: Observational evidence and a minimal theory of bimodality, *Q. J. R. Meteorolog. Soc.*, *112*, 661–674, doi:10.1002/qj.49711247306.

Benzi, R., and A. Speranza (1989), Statistical properties of low-frequency variability in the Northern Hemisphere, *J. Clim.*, *2*, 367–379, doi:10.1175/1520-0442(1989)002<0367:SPOLFV>2.0.CO;2.

Blackmon, M. (1976), A climatological spectral study of 500 mb geopotential height of Northern Hemisphere, *J. Atmos. Sci.*, *33*, 1607–1623, doi:10.1175/1520-0469(1976)033<1607:ACSSOT>2.0.CO;2.

Chang, E. K. M. (2012), CMIP5 multimodel ensemble projection of storm track change under global warming, *J. Geophys. Res.*, *117*, D23118, doi:10.1029/2012JD018578.

Chang, E. K. M. (2013), Impacts of background field removal on CMIP5 projected changes in Pacific winter cyclone activity, *J. Geophys. Res. Atmos.*, doi:10.1002/2013JD020746, in press.

Charney, J., and D. Straus (1980), Form-drag instability, multiple equilibria and propagating planetary waves in baroclinic, orographically forced, planetary wave systems, *J. Atmos. Sci.*, *37*(6), 1157–1176.

Charney, J., and J. De Vore (1979), Multiple flow equilibria in the atmosphere and blocking, *J. Atmos. Sci.*, *36*, 1205–1216, doi:10.1175/1520-0469(1979)036<1205:MFEITA>2.0.CO;2.

Colle, B., Z. Zhang, K. Lombardo, E. Chang, P. Liu, and Zhang M. (2013), Historical evaluation and future prediction of eastern North America and western Atlantic extratropical cyclones in the CMIP5 models during the cool season, *J. Clim.*, *26*, 6882–6903, doi:10.1175/JCLI-D-12-00498.1.

Czaja, A., and J. Marshall (2006), The partitioning of poleward heat transport between the atmosphere and ocean, *J. Atmos. Sci.*, *63*, 1498–1511, doi:10.1175/JAS3695.1.

Dee, D. P., et al. (2011), The ERA-Interim reanalysis: Configuration and performance of the data assimilation system, *Q. J. R. Meteorolog. Soc.*, *137*, 553–597.

Dell'Aquila, A., V. Lucarini, P. Ruti, and S. Calmanti (2005), Hayashi spectra of the Northern Hemisphere mid-latitude atmospheric variability in the NCEP-NCAR and ECMWF reanalyses, *Clim. Dyn.*, *25*, 1639–652, doi:10.1007/s00382-005-0048-x.

Fraedrich, K., and H. Bottger (1978), A wavenumber-frequency analysis of the 500 mb geopotential at 50°N, *J. Atmos. Sci.*, *35*, 745–750, doi:10.1175/1520-0469(1978)035<0745:AWFAOT>2.0.CO;2.

Hayashi, Y. (1979), A generalized method of resolving transient disturbances into standing and travelling waves by space-time spectral analysis, *J. Atmos. Sci.*, *36*, 1017–1029, doi:10.1175/1520-0469(1979)036<1017:AGMORT>2.0.CO;2.

Kistler R., et al. (2001), The NCEP-NCAR 50-year reanalysis: Monthly means CD-ROM and documentation, *Bull. Am. Meteorol. Soc.*, *82*(2), 247–267.

Knutti, R., and J. Sedláček (2012), Robustness and uncertainties in the new CMIP5 climate model projections, *Nat. Clim. Change*, *3*, 369–373, doi:10.1038/nclimate1716.

Knutti, R., D. Masson, and A. Gettelman (2013), Climate model genealogy: Generation CMIP5 and how we got there, *Geophys. Res. Lett.*, *36*, 1194–1199, doi:10.1002/grl.50256.

Lucarini, V., S. Calmanti, A. Dell'Aquila, P. M. Ruti, and A. Speranza (2007), Intercomparison of the Northern Hemisphere winter midlatitude atmospheric variability of the IPCC models, *Clim. Dyn.*, *28*, 829–848, doi:10.1007/s00382-006-0213-x.

Lucarini, V., and F. Ragone (2011), Energetics of climate models: Net energy balance and meridional enthalpy transport, *Rev. Geophys.*, *49*, RG1001, doi:10.1029/2009RG000323.

Mizuta, R. (2012), Intensification of extratropical cyclones associated with the polar jet change in the CMIP5 global warming projections, *Geophys. Res. Lett.*, *39*, L19707, doi:10.1029/2012GL053032.

Pratt, R. W. (1976), The interpretation of space-time spectral quantities, *J. Atmos. Sci.*, *33*, 1060–1066, doi:10.1175/1520-0469(1976)033<1060:TIOSTS>2.0.CO;2.

Ruti, P., V. Lucarini, A. Dell'Aquila, S. Calmanti, and A. Speranza (2006), Does the subtropical jet catalyze the midlatitude atmospheric regimes?, *Geophys. Res. Lett.*, *33*, L06814, doi:10.1029/2005GL024620.

Speranza, A. (1983), Deterministic and statistical properties of the westerlies, *Pure Appl. Geophys.*, *121*, 511–562, doi:10.1007/BF02590154.

Taylor, K., R. Stouffer, and G. Meehl (2012), An overview of CMIP5 and the experiment design, *Bull. Am. Meteorol. Soc.*, *93*, 485–498, doi:10.1175/BAMS-D-11-00094.1.

Tibaldi, S. (1986), Envelope orography and maintenance of the quasi-stationary circulation in the ECMWF global models, *Adv. Geophys.*, *29*, 339–373, doi:10.1016/S0065-2687(08)60045-X.

Wallace, J., S. Tibaldi, and A. Simmons (1983), Reduction of systematic forecast errors in the ECMWF model through the introduction of an envelope orography, *Q. J. R. Meteorolog. Soc.*, *109*, 683–717, doi:10.1002/qj.49710946202.

Zappa, G., L. C. Shaffrey, K. I. Hodges, P. G. Sansom, and D. B. Stephenson (2013), A multimodel assessment of future projections of North Atlantic and European extratropical cyclones in the CMIP5 climate models, *J. Climate*, *26*, 5846–5862.

Zappa, G., L. C. Shaffrey, and K. I. Hodges (2013), The ability of CMIP5 models to simulate the North Atlantic extratropical cyclones, *J. Climate*, *26*, 5846–5862.

  